

Latitudinal variation of the balance between plankton photosynthesis and respiration in the eastern Atlantic Ocean

Pablo Serret¹ and Carol Robinson

Plymouth Marine Laboratory, Prospect Place, West Hoe, Plymouth PL1 3DH, United Kingdom

Emilio Fernández and Eva Teira

Universidad de Vigo, Departamento de Ecología y Biología Animal, 36200 Vigo, Spain

Gavin Tilstone²

Instituto de Investigaciones Marinas-C.S.I.C., c/Eduardo Cabello, 6, 36208 Vigo, Spain

Abstract

A knowledge of the balance between plankton gross primary production (GPP) and community respiration (CR) in the open ocean is vital to the accurate determination of the global carbon cycle, yet the paucity of open ocean measurements severely limits our understanding. This study measured GPP, net community production, dark CR, and size-fractionated primary production in the upper 200 m of a 12,100 km latitudinal (32°S–48°N) transect in the Eastern Atlantic Ocean during May and June 1998. This comprehensive data set, which spans five contrasting plankton regimes, including two open ocean oligotrophic provinces, is used to derive a GPP:CR relationship, which suggests that net heterotrophy ($GPP < CR$) prevails in the eastern Atlantic when primary production falls below $\sim 100 \text{ mmol O}_2 \text{ m}^{-2} \text{ d}^{-1}$. The predictive capability of this relationship is compared with that of the only other published relationship based on similar methodologies and is found to give a more representative description of the autotrophic ($GPP > CR$) to heterotrophic seasonal cycle in the Bay of Biscay. This improved predictive power is attributed to the increased representativeness of the current data set. Specifically, the interpretation suggests that the influence of community structure on net ecosystem metabolism implies that prediction of GPP:CR balances in pelagic ecosystems can be best achieved by use of a data set that covers a wide range of community structure and not only a wide range in the magnitude of primary production.

The significant contribution of the marine biota to the global carbon cycle (e.g., Sarmiento and Siegenthaler 1992) ultimately results from the balance between gross primary production (GPP) (all photosynthesis independent of its fate) and community respiration (CR) (the oxidative consumption of organic matter by autotrophic and heterotrophic organ-

isms). Quantification of such a balance (net community production, $NCP = GPP - CR$) in the open ocean is hampered by the poor marine CR database, the question as to what each analytical technique measures in terms of GPP or net primary production ($NPP = GPP$ minus algal respiration) (Williams 1993), and the time-consuming methods available for directly measuring NCP. Existing global estimates therefore rely on empirical relationships between the magnitudes of GPP (Williams 1998) or NPP (del Giorgio et al. 1997) (derived from ΔO_2 or ^{14}C techniques), and bacterial (del Giorgio et al. 1997) or total CR (Duarte and Agustí 1998; Williams 1998; Duarte et al. 1999) to predict NCP where only primary production data are available. These studies disagree by about one order of magnitude on the predicted rate of GPP at which CR exceeds GPP ($GPP \sim 1 \text{ mmol O}_2 \text{ m}^{-3} \text{ d}^{-1}$ vs. $GPP = 16.7 \text{ mmol O}_2 \text{ m}^{-2} \text{ d}^{-1}$), which has generated an active debate on the net metabolism of open ocean unproductive ecosystems. The conflicting conclusions that (1) microbial respiration exceeds photosynthesis in unproductive aquatic systems (del Giorgio et al. 1997; Duarte and Agustí 1998) and (2) the open ocean is in metabolic balance (Williams 1998) have been questioned on the basis of the inadequacy of the data sets (Geider 1997; but see also del Giorgio and Cole 1997; Williams 1998; Duarte et al. 1999) and the form of data analysis (Duarte et al. 1999; Williams and Bowers 1999). However, the paucity of NCP measurements in the oligotrophic open ocean has prevented an independent test of either of these models.

¹ Corresponding author (pserret@uvigo.es). Present address: Universidad de Vigo, Departamento de Ecología y Biología Animal, 36200 Vigo, Spain.

² Present address: Plymouth Marine Laboratory, Prospect Place, West Hoe, Plymouth PL1 3DH, United Kingdom.

Acknowledgments

We thank I. Joint, P. J. le B. Williams, C. M. Duarte, and R. Menéndez for constructive comments on a draft of a previous version of this manuscript. We are indebted to the principal scientist, J. Aiken, and personnel on board *RRS James Clark Ross* during the AMT-6 cruise. Thanks to P. J. le B. Williams for the generous loan of analytical equipment. SeaWiFS data courtesy of the NASA SeaWiFS Project and Orbital Sciences Corporation. We acknowledge S. Lavender, Remote Sensing Group, PML, for image analysis. Thanks to B. G. Castro and J. I. Lorenzo for advice on statistics. P.S. was funded by an EU Marie Curie Research Training Grant, and C.R. was funded by a NERC Advanced Research Fellowship (GT5/96/8/MS). E.T. and E.F. were funded by MEC grant MAR98-1417E and the EU contract CANIGO (MAS3CT960060). G.H.T. was supported by a fellowship from the European Commission MAST programme (MAS3-CT96-5022). This is contribution number 52 of the AMT programme (<http://www.pml.ac.uk/amt/index.html>). Comments by three anonymous referees have improved this work.

So far, GPP:CR relationships have been obtained by aggregating independent data from different times and locations, without explicit attention to the state or type of community studied. One implicit assumption is the prevalence of steady-state conditions during each sampling period—that is, that the connection between the processes of production and consumption of organic matter occurs locally in both space and time. Although Williams (1998) highlighted the importance of using depth-integrated data of GPP and CR to account for the compensation of imbalances over the water column, current published GPP:CR relationships do not explicitly incorporate an analysis of the horizontal or temporal scales involved. However, accumulation of dissolved organic matter (DOM) in the upper mixed layer (see Hansell and Carlson 1998) may give rise to the linkage of production and consumption of organic matter over large spatial or long temporal scales (e.g., Pomeroy and Wiebe 1993; Sherr and Sherr 1996), thus affecting the GPP:CR balance at local scales, as shown in seasonal temperate systems (e.g., Blight et al. 1995; Serret et al. 1999).

In addition, the relationship between GPP and CR may not only be different over different spatial and temporal scales, but, more important, it will probably differ between systems near equilibrium and those that are transient (Burke et al. 1997). In practice, given the imprecise nature of the concept of *equilibrium* in ecology, and especially in pelagic systems, and the extreme difficulty in addressing the large time- and space scales of trophic functioning, the critical point is to ensure that data are *representative* of the functional community—that is, that they characterize long-term averages (Hairston and Hairston 1993).

Even if the data used are representative, the simple use of GPP:CR relationships to estimate *trophic status* (i.e., the GPP:CR balance at ecologically significant scales; e.g., Smith and Hollibaugh 1997 and references therein) assumes that the degree of heterotrophy of pelagic ecosystems may be predicted from their total amount of GPP, which overlooks the influence of food web structure on net ecosystem metabolism. However, the net balance of an ecosystem must be dependent not only on the total amount of GPP but also on the type and activity of the community of heterotrophs that such production sustains (Hairston and Hairston 1993; McGrady-Steed et al. 1997; Petchey et al. 1999). If food web organization, and not only primary production, influences the degree of heterotrophy of the pelagic ecosystems, the variation of CR with GPP may be different when analyzed within or between different communities. Consequently, generalized GPP:CR relationships might be dependent on the range of different communities studied and not only on the range of GPP.

We present here data of GPP and CR in the euphotic zone of five biogeochemical provinces of the eastern Atlantic Ocean in the austral spring-to-summer transition period, providing new empirical evidence of the GPP:CR balance in two open ocean oligotrophic habitats. This data set allows us to explore the regional variability of net community production, but, more important, because it is representative of contrasting plankton regimes, it also enables us to investigate the influence of the type of plankton community on GPP:CR balances.

Materials and Methods

Sampling—A latitudinal (32°S–48°N) transect across the Eastern Atlantic Ocean (Atlantic Meridional Transect [AMT]–6 cruise; see Aiken et al. 2000) was conducted on board *RRS James Clark Ross* on passage between Cape Town, South Africa, and Grimsby, United Kingdom (15 May–16 June 1998) (Fig. 1); 24 stations were sampled daily (between 08:00 and 09:00 GMT) at ~320 km intervals. Vertical profiles of temperature and conductivity were performed by use of a Seabird 911+ conductivity-temperature-depth (CTD) rosette fitted to a rosette of 12 × 30 liter Niskin-type sampling bottles. Vertical profiles of photosynthetically active irradiance (400–700 nm) were calculated by integrating the measurements of downwelling irradiance at seven SeaWiFS wavelength bands derived from daily casts of an optical profiler (SeaOPS) and a free-fall optical profiler (SeaFALLS) (Aiken et al. 2000). Water was collected from 9–12 depths in the upper 200 m.

Dissolved oxygen—A 60-cm³ gravimetrically calibrated, borosilicate glass bottle was carefully filled from each Niskin bottle by use of silicon tubing. Measurements of dissolved oxygen were made with an automated Winkler titration system based on that described in Williams and Jenkinson (1982). Oxygen saturation was calculated by use of the equations for the solubility of oxygen in seawater of Benson and Krause (1984).

Size-fractionated chlorophyll *a* concentration—A total of 200–300 cm³ water samples were sequentially filtered through 20, 2, and 0.2 μm pore size polycarbonate filters. Chl *a* was extracted from the filters in 90% acetone at –20°C for 12–24 h and measured by use of a Turner 10-AU fluorometer calibrated against Chl *a* standards (Sigma).

Size-fractionated and total particulate organic carbon production (PO¹⁴CP) rates—At each station, samples were collected from each of seven depths corresponding to optical depths ranging from 97% to 1% of surface irradiance. Water from each depth was distributed into four 75-cm³ acid-cleaned polypropylene bottles (three transparent and one dark). Each bottle was inoculated with 185–370 KBq (5 to 10 μCi) NaH¹⁴CO₃ and then incubated for 6–7 h in an on-deck incubator that simulated the irradiance at the original sampling depths by use of various combinations of neutral density and blue plastic filters. A previous comparison of this on-deck incubation procedure and an in situ incubation technique found no statistical difference between the respective ¹⁴C derived estimates of primary production (Joint et al. 1993). After the incubation period, samples were filtered at very low vacuum (<50 mm Hg) through 0.2, 2, and 20 μm polycarbonate filters. Filters were then fumed with concentrated HCl for 12 h. Radioactivity was measured with a Beckman LS6000 SC scintillation counter. Quenching was corrected by use of an external standard. Total primary production was determined by summing the integrated size fractionated rates. Following the method of Marañón et al. (2000), the hourly production rates were converted to daily rates by taking into account the length of daylight and as-

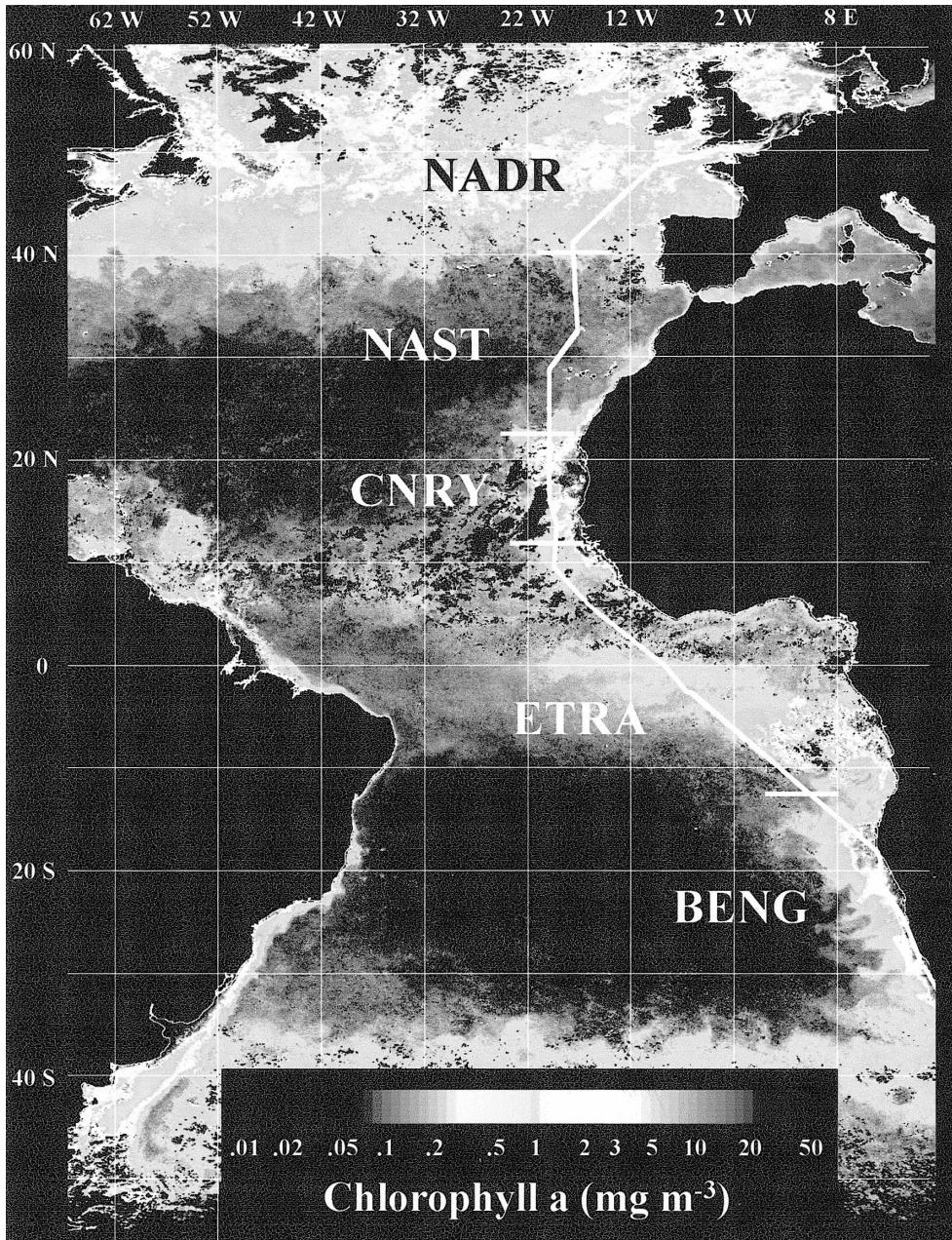


Fig. 1. Cruise track overlaid over SeaWiFS Chl *a* May monthly composite image. The approximate boundaries of the five biogeochemical provinces (Longhurst 1998) traversed are shown: BENG, ETRA, CNRY, NAST-E, and NADR.

suming that dark respiratory losses represent 20% of light PO^4CP (see also review by Geider 1992).

GPP, NCP, and dark CR—GPP, NCP, and dark CR (DCR) were determined from in vitro changes in dissolved oxygen after 24-h light and dark bottle incubations. Water samples (25 dm^3) were collected each day from the CTD rosette into acid-washed opaque polypropylene aspirators from depths equivalent to 97%, 33%, and 1% of surface irradiance. Water was siphoned from each 25 dm^3 opaque aspirator into $15 \times 60\text{ cm}^3$ borosilicate glass bottles through silicon tubing. From each depth, five replicate bottles were fixed immedi-

ately, five bottles were kept in darkness, and five bottles were incubated under irradiance conditions that simulated those of the original sampling depth, as described above. Samples collected from depths at which in situ temperature was $>5^\circ\text{C}$ lower than surface water temperature were also incubated in the dark in temperature controlled water baths at near in situ temperature for 24 h. In these instances, reported DCR rates correspond to those measured at about in situ temperature, whereas most GPP were discarded. Only seven of these GPP data from $\sim 40\text{--}75\text{ m}$ depth in the area of the Guinea Dome (between $\sim 3^\circ\text{N}$ and 13°N) are included after detailed comparison with Chl *a* concentration and

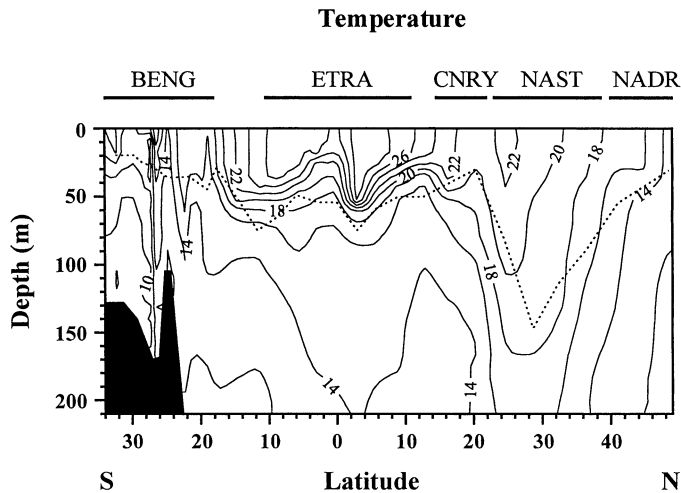


Fig. 2. Spatial distribution of temperature ($^{\circ}\text{C}$) along the AMT-6 transect. Dotted line, euphotic depth.

PO^{14}CP rates. After the incubation period, dissolved oxygen concentration was determined following the method described above. Production and respiration rates were calculated from the difference between the means of the replicate light and dark incubated and zero time analyses: $\text{NCP} = \text{measured } \Delta\text{O}_2 \text{ in light bottles (mean of } [\text{O}_2] \text{ in 24-hr light} - \text{mean initial } [\text{O}_2])$; $\text{DCR} = \text{measured } \Delta\text{O}_2 \text{ in dark bottles (mean initial } [\text{O}_2] - \text{mean } [\text{O}_2] \text{ in 24-hr dark)}$; $\text{GPP} = \text{NCP} + \text{DCR}$. Euphotic zone integrated values were obtained by trapezoidal integration of the volumetric data down to the depth of 1% surface incident irradiance. Following the method of Miller and Miller (1988), we calculated the standard deviation of integrated NCP through propagation of the random error in the volumetric measurements as $\sigma_{\text{integral}} = \frac{1}{2}\sqrt{[\sum (z_{i+1} - z_i)^2(\sigma_{i+1}^2 + \sigma_i^2)]}$, where σ is the SD, z is the sampled depth, and i is the depth level. Euphotic depth ranged from ~ 30 m in the Benguela Current Coastal Province (BENG) to >100 m in the North Atlantic Subtropical Gyre.

Results

Individual data of temperature, salinity, dissolved oxygen, and Chl *a* concentrations, PO^{14}CP rates, percentage of PO^{14}CP by cells $<2 \mu\text{m}$, and GPP, DCR, and NCP rates at every sampled station are available in Web Appendix 1 on the L&O website at http://www.aslo.org/lo/toc/vol46/issue_7/1642a1.pdf.

Water column thermal structure—The spatial distribution of temperature (Fig. 2) reflects the hydrographic characteristics of the different provinces traversed during the cruise: BENG, Eastern Tropical Atlantic Province (ETRA), Eastern (Canary) Coastal Province (CNRY), North Atlantic Subtropical Gyral Province (NAST-E), and North Atlantic Drift Province (NADR) (Longhurst 1998), sampled during the spring-to-summer transition period.

In the southernmost part of the transect, the upwelling system in the BENG ($\sim 33^{\circ}\text{S}$ – 18°S) is shown by the tilting

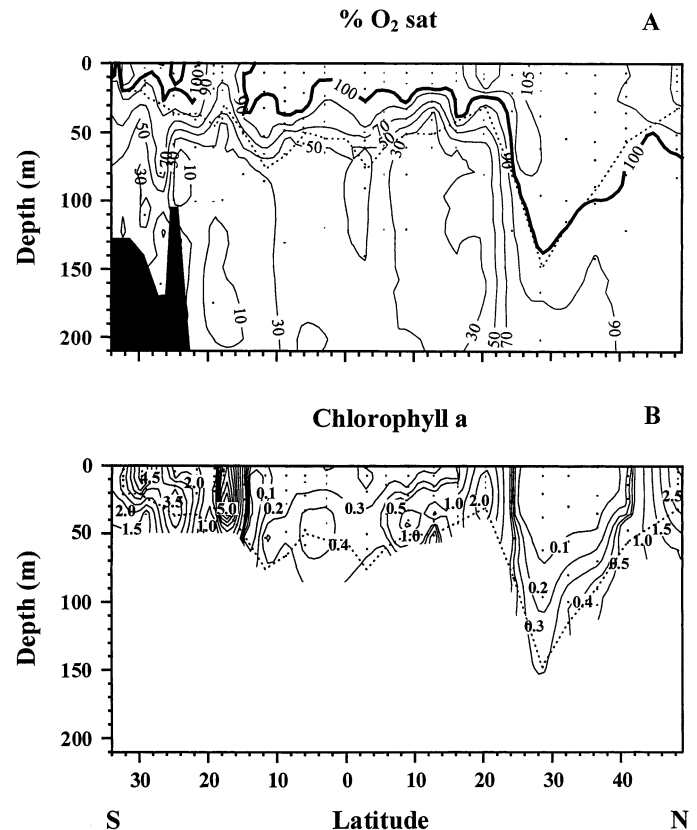


Fig. 3. Spatial distribution of (A) the percentage of oxygen saturation and (B) Chl *a* concentration (mg m^{-3}) along the AMT-6 transect. Dotted line, euphotic depth.

of the isotherms. Areas of intense upwelling, with surface temperature $<15^{\circ}\text{C}$, were found close to areas of relaxed upwelling or convergence, which reflects the highly dynamic characteristics of this coastal regime (e.g., Luthjermams and Meeuwis 1987). A sharp hydrographic front, located at $\sim 16^{\circ}\text{S}$ – 12°S , separated the mixed waters of the BENG from the strongly stratified waters of the ETRA. The Angola-Benguela Front (e.g., Shannon et al. 1987) is regarded as the convergence zone between the cold northward-flowing Benguela Current and the warm southward-flowing Angola Current. Several distinct hydrographic features can be seen in the ETRA ($\sim 10^{\circ}\text{S}$ – 11°N) (see Longhurst 1998; Stramma and Schott 1999; and references therein): in the tropical cyclonic Angola Gyre, centered $\sim 8^{\circ}\text{S}$, a sharp and relatively shallow thermocline (~ 50 m) was observed. The depth of the middle thermocline (corresponding roughly to the 21°C isotherm) decreased from 50 to ~ 30 m at the equatorial divergence. North of the Equator (3°N), the northern tropical convergence lying between the South Equatorial Current and the North Equatorial Counter Current (Guinea Current) can be seen in the compression and deepening of the thermocline down to ~ 60 m depth. Further north, through the North Equatorial Counter Current, surface temperature and the depth of the thermocline progressively decreased, reaching the minimum at the Guinea Dome (at $\sim 12^{\circ}\text{N}$). The relatively shallow thermocline throughout the ETRA (17°C isotherm above 65 m depth) is characteristic of this tropical area dur-

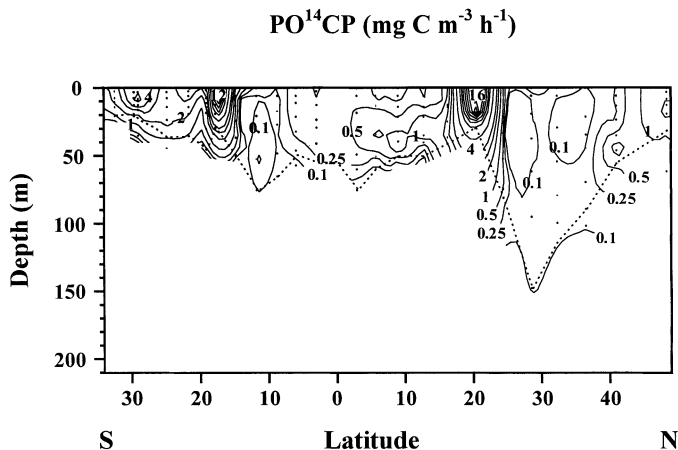


Fig. 4. Spatial distribution of total particulate organic carbon production along the AMT-6 transect. Dotted line, euphotic depth.

ing the southern autumn-winter, resulting from the intensification of the Trade Winds (Longhurst 1998 and references therein). To the north of the ETRA, the cruise track approached the northwestern African coast, entering the CNRY province ($\sim 15\text{--}23^\circ\text{N}$) (Longhurst 1998), where coastal upwelling was evident in both the tilting of the isotherms at 20°N and the spatial distribution of surface Chl *a* (see Fig. 1). Northward of $\sim 23^\circ\text{N}$, as the track moved away from the African coast, the interface with the NAST-E province was identified by the spreading of the thermocline and the deepening of the upper mixed layer down to >100 m depth. A broad frontal zone north of $\sim 37^\circ\text{N}$ marked the transition from the NAST-E to the cooler and less saline waters of the NADR, where a shallower (<50 m) thermocline was observed. In the northernmost part of the transect (at $\sim 48^\circ\text{N}$), the thermocline tilted at the European shelf break upwelling.

Oxygen saturation and Chl *a* concentration—Figure 3 shows the spatial variability of the percentage of oxygen saturation ($\%O_2$ sat) and Chl *a* concentration along the AMT6 transect. The $\%O_2$ sat in the upper ocean is a valuable tool for broadly summarizing the recent history of biological activity (e.g., Chapman and Shannon 1985; Najjar and Keeling 1997). High levels of O_2 sat ($>105\%$) and Chl *a* (>1 mg m^{-3}) were observed near the surface in both temperate waters and coastal upwelling systems (BENG and CNRY). The latter also exhibited low O_2 sat in subsurface waters, thereby causing the strong vertical oxygen gradients characteristic of these systems (Chapman and Shannon 1985). Some stations in the north BENG (e.g., $\sim 25^\circ\text{S}$) and south of the CNRY presented subsurface Chl *a* maxima and very low levels of O_2 sat ($<30\%$) in subsurface waters. The N BENG was the only region where O_2 sat $<100\%$ was found at the surface of strongly upwelled stations. The highest phytoplankton biomass was found at the northern end of this region, near the frontal zone between the BENG and ETRA. Both oligotrophic provinces (ETRA and NAST-E) exhibited low phytoplankton biomass, subsurface Chl *a* maxima (DCM), and $\%O_2$ sat $>100\%$ through the surface mixed layer. The location of the DCM at the base of the euphotic layer and its Chl *a* concentration ($\sim 0.2\text{--}0.4$ mg m^{-3}) are charac-

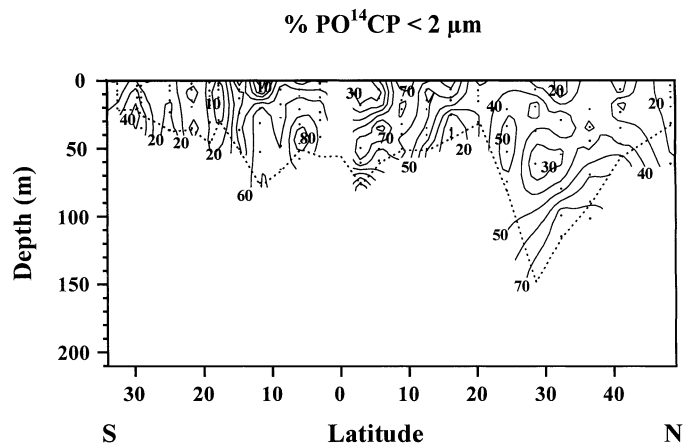


Fig. 5. Spatial distribution of the percentage of particulate organic carbon production by cells <2 μm along the AMT-6 transect. Dotted line, euphotic depth.

teristic of low latitudes in the Atlantic Ocean (e.g., Mara $\tilde{\text{n}}\text{o}n$ et al. 2000 and references therein). Oxygen saturation did not show any relation to the DCM. Both the thermocline and the DCM were shallower in the ETRA, where strong vertical oxygen gradients were observed ($<50\%$ O_2 sat below the thermocline). The lowest deep oxygen content and highest Chl *a* concentration in this region were observed in the area of the Guinea Dome (Oudot 1989). North of $\sim 25^\circ\text{N}$, a marked increase in deep oxygen content was observed.

Total and size-fractionated particulate organic carbon production ($PO^{14}CP$)—The latitudinal distribution of total particulate primary production (Fig. 4) resembles that of Chl *a*, whereas the relative dominance of picoplankton (Fig. 5) tended to decrease with the productivity of the province. Higher values of $PO^{14}CP$ were measured in the Chl *a*-rich waters of the coastal upwelling regions of BENG and CNRY and in temperate waters. In the BENG and CNRY provinces, the highest $PO^{14}CP$ rates were always found near the surface at stations with low surface temperature and high surface Chl *a* concentration, whereas stations with relatively higher surface temperature and subsurface Chl *a* maxima (e.g., $\sim 25^\circ\text{S}$) had low $PO^{14}CP$ rates throughout the water column. The contribution of picoplankton to total primary production was always very low in areas of high phytoplankton biomass, both at the surface productive and subsurface unproductive Chl *a* maxima. The ranges of both Chl *a* concentration ($\sim 55\text{--}150$ mg m^{-2}) and $PO^{14}CP$ rates ($\sim 0.3\text{--}3$ $\text{g C m}^{-2} \text{d}^{-1}$) measured in the BENG, as well as their distribution in relation to hydrographic conditions, are consistent with studies of the hydrodynamic control of phytoplankton patchiness and growth in this system (e.g., Shannon and Pillar 1986; Pitcher et al. 1992). Similarly, values measured at the CNRY stations ($\sim 0.4\text{--}2$ mg Chl a m^{-3} in the surface; $\sim 0.7\text{--}2.5$ $\text{g C m}^{-2} \text{d}^{-1}$) are representative of mesotrophic and eutrophic conditions, respectively, in this province (Morel et al. 1996).

Although in the northern ETRA, subsurface maxima of $PO^{14}CP$ were observed that corresponded to the vertical distribution of Chl *a*, south of the Equator, no increase in $PO^{14}CP$ rates was seen in relation to the DCM. In contrast

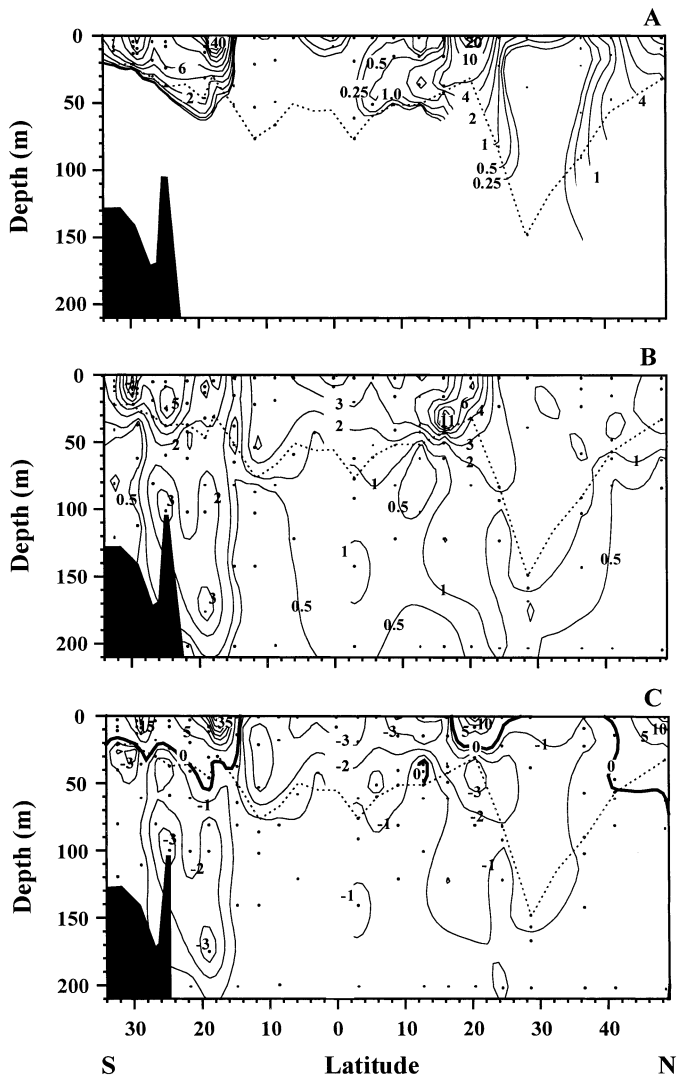


Fig. 6. Spatial distribution of (A) GPP ($\text{mmol O}_2 \text{ m}^{-3} \text{ d}^{-1}$) and (B) DCR ($\text{mmol O}_2 \text{ m}^{-3} \text{ d}^{-1}$). Panel (C) combines the balance between GPP and DCR (NCP) in the euphotic zone, together with DCR measurements below the 1% light level. Dotted line, euphotic depth.

to upwelling provinces, in the ETRA, the relative contribution of picoplankton to total primary production increased with productivity and especially with phytoplankton biomass. In both the northern and southern part of the province, >60% of the primary production was attributable to cells <math> < 2 \mu\text{m}</math> when Chl *a* concentration was >math> > 0.3 \text{ mg m}^{-3}</math>. Throughout the ETRA, low levels of surface Chl *a* ($\sim 0.2 \text{ mg m}^{-3}$), relatively deep ($\sim 40 \text{ m}$) Chl *a* maxima, and low primary production ($\sim 40\text{--}350 \text{ mg C m}^{-2} \text{ d}^{-1}$) suggest that our sampling occurred prior to the development of the characteristic summer pelagic bloom in this province (Longhurst 1998).

In the NAST-E, very low PO^{14}CP rates were measured, with values only exceeding $0.1 \text{ mg C m}^{-3} \text{ h}^{-1}$ near the surface and in deep waters ($\sim 60\text{--}110 \text{ m}$). The percentage of total primary production attributable to picoplankton increased with depth, reaching >70% in the DCM. Integrated

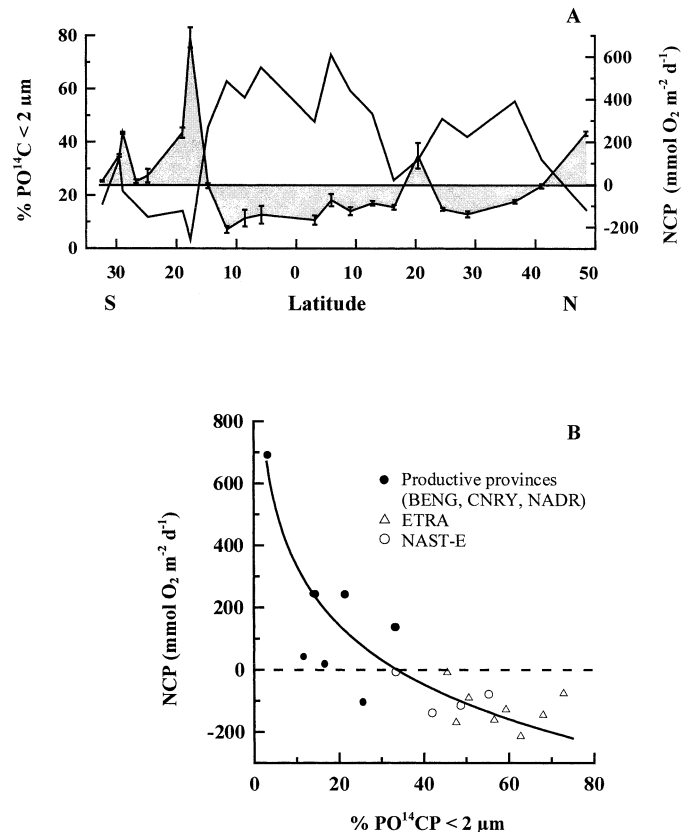


Fig. 7. (A) Latitudinal distribution of euphotic zone integrated percentage of particulate organic carbon production by cells <math> < 2 \mu\text{m}</math> (solid line) and NCP (shaded trend; \pm SD) along the AMT-6 transect. (B) Relationship between euphotic zone integrated percentage of particulate carbon incorporated by phytoplankton <math> < 2 \mu\text{m}</math> and integrated NCP in five biogeochemical provinces of the eastern Atlantic Ocean. The intersection of the reduced major axis (solid line; $\text{NCP} = -276.5 \log [\% \text{PO}^{14}\text{CP} < 2 \mu\text{m}] + 972.9$, $r^2 = 0.761$, $n = 21$, $P < 0.0001$) with the line of $\text{NCP} = 0$ (dashed line) is at 33% $\text{PO}^{14}\text{CP} < 2 \mu\text{m}$. Note that the range of $\% \text{PO}^{14}\text{CP} < 2 \mu\text{m}$ (<math> < 5\%</math> to >math> > 70\%</math>) covers the full spectrum of community structures.

values of PO^{14}CP of $\sim 370 \text{ mg C m}^{-2} \text{ d}^{-1}$ were measured at stations near the boundaries of this province, whereas $\sim 150 \text{ mg C m}^{-2} \text{ d}^{-1}$ characterized the stations with the deepest mixed layer and DCM. These values are within the range of those reported by Marañón et al. (2000) for this region and agree with those measured during the low production season at Bermuda (NAST-W) (Michaels and Knap 1996), being slightly lower than those reported by Morel et al. (1996) for the tropical northeast Atlantic at 20°N , 30°W .

PO^{14}CP rates increased in the NADR province, where, corresponding to the distribution of Chl *a*, a subsurface production maximum was observed in the southernmost station, whereas higher surface rates were measured at the European shelf break. In this productive region, as in the BENG and CNRY upwellings, and contrary to the unproductive ETRA and NAST, the relative contribution of picoplankton to total primary production decreased with productivity.

Plankton oxygen production and consumption—The range of gross production of oxygen by phytoplankton (GPP) was

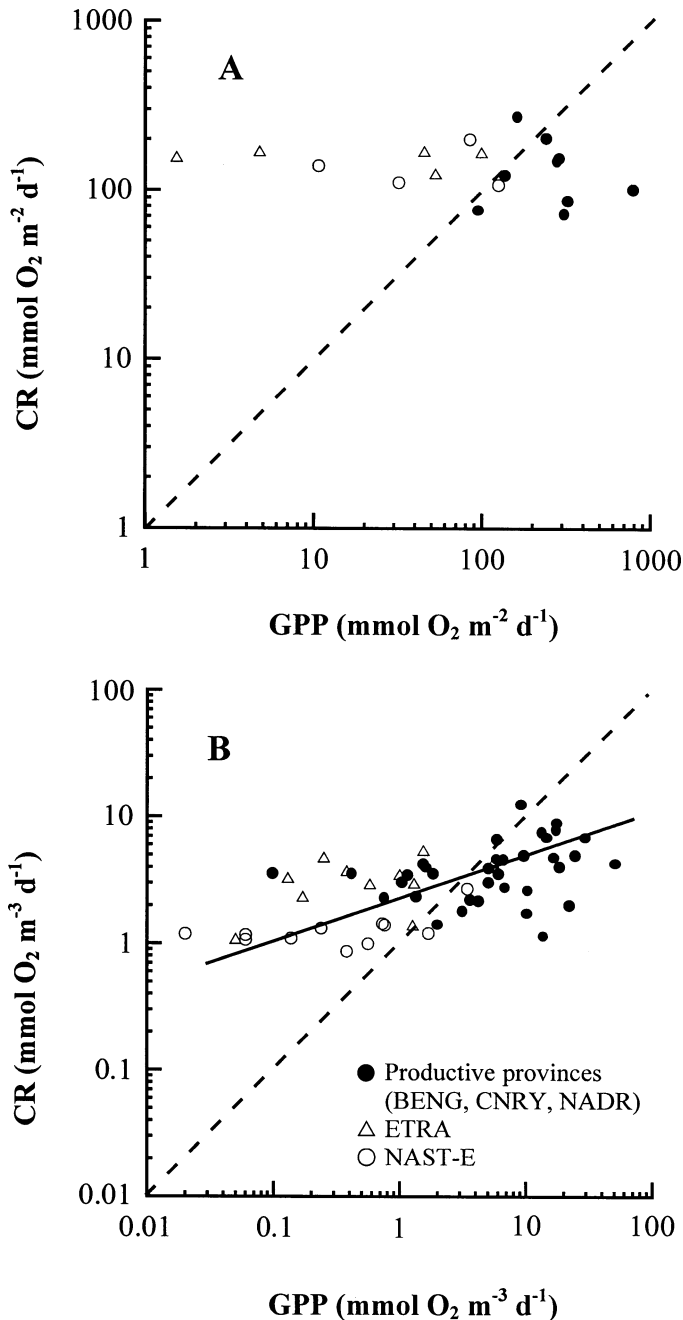


Fig. 8. Relationship between GPP and DCR rates. The average percentage of integrated primary production by cells $<2 \mu\text{m}$ was $19\% \pm 3\%$ in productive regions, $58\% \pm 3\%$ in ETRA, and $45\% \pm 4\%$ in NAST-E. (A) Euphotic zone integrated data. (B) Volumetric data. The solid line is the reduced major axis ($\text{DCR} = 2.284 \text{GPP}^{0.341}$, $n = 57$, $r^2 = 0.321$, $P < 0.001$), and the dashed ones are the 1:1 lines.

about four times that of DCR (Fig. 6A,B). GPP and DCR were not directly related, although both exhibited patterns related to the distribution of Chl *a*. High surface values of GPP were measured in surface Chl *a*-rich waters, but an increase of GPP at the DCM of oligotrophic provinces was only detected in the northern ETRA. A subsurface GPP maximum was also observed south of the CNRY upwelling re-

gion. On the contrary, the highest DCR rates were measured not in the most productive waters but in the low productive DCM observed at some stations of the BENG and CNRY upwellings. Throughout both oligotrophic provinces, and especially in the ETRA, relatively high DCR rates ($>1 \text{mmol O}_2 \text{m}^{-3} \text{d}^{-1}$) were measured in the unproductive, O₂-supersaturated waters of the upper mixed layer. In these provinces, no relationship was found between the vertical distribution of DCR rates and the DCM.

Figure 6C combines the balance between GPP and DCR (NCP) in the euphotic zone, together with DCR measurements below the 1% light level; i.e., under the assumption that GPP is negligible below the euphotic layer (hence $\text{NCP} = -\text{DCR}$), it depicts the spatial variability of NCP in the upper 200 m. Within the euphotic zone, NCP was only positive in the productive surface waters of the upwelling and frontal regions, which were rich in Chl *a* and supersaturated with respect to O₂, and where phytoplankton production was dominated by larger cells ($>2 \mu\text{m}$). As with GPP, the latitudinal variability of surface NCP was related to that of surface Chl *a*. In both oligotrophic provinces, NCP was consistently negative in the euphotic zone throughout the region. Higher negative values were found in the ETRA, where Chl *a* and PO¹⁴CP were also higher (Figs. 1, 3B, and 4) and the thermocline shallower (Fig. 2). In the NAST-E province, positive NCP was only measured in the relatively productive surface waters of the stations sampled near its boundaries.

In productive provinces, higher NCP was usually found in areas of elevated %O₂ sat (see Figs. 3A and 6), despite the distributions of biomass and PO¹⁴CP rates in these provinces being governed by the highly dynamic coastal upwellings and fronts (see above and, e.g., Pitcher et al. 1992). A similar trend exists in the spatial distribution of NCP and %O₂ sat in the upper 200 m. Such a correspondence suggests a tight and rapid recycling of the organic matter produced locally. This contrasts with the situation in oligotrophic provinces, where negative NCP was always measured together with O₂ supersaturation in the upper waters. A similar maintenance of O₂ supersaturation with net heterotrophy was observed in the euphotic zone of the stratified oligotrophic waters of the southern Bay of Biscay during the summer (Serret et al. 1999), which is consistent with a slow consumption of organic matter previously synthesized in the same water and highlights the differences in timescale of estimations of net community metabolism based on in vitro oxygen fluxes and in situ concentration. In the ETRA region, where both NCP and the %O₂ sat exhibited stronger vertical gradients, not related to the subsurface Chl *a* maxima, an inverse relationship was found between these two variables.

Discussion

Data representativeness: the linkage between trophic dynamics and community structure—It is critical that the data used to derive meaningful GPP:CR relationships and to understand the functioning of an ecosystem, are representative of long-term averages (see Hairston and Hairston 1993). The biomass and activity of heterotrophs in a community are not only sustained by locally produced organic matter nor ex-

clusively controlled by substrate availability. Consequently, such activity is not always directly related to the concurrent activity of autotrophs (e.g., early or late spring bloom), and hence the relationship between GPP and CR in a transient community will not necessarily reflect the trophic dynamics of the ecosystem. Similarly, the relative abundance of the different species sharing an habitat at a certain time will not necessarily reflect the structure of the community or the organization of the food web. The obvious difficulty we face is the assessment of the representativeness of a set of instantaneous measurements without actually knowing the long term averages.

Various theoretical (e.g., Legendre and Lefevre 1991; Moloney and Field 1991; Kiørboe 1993) and field studies (e.g., Legendre et al. 1993; Nielsen and Hansen 1995; Pesant et al. 1998; Tamigneaux et al. 1999) have shown that the structure of a plankton community close to equilibrium can be predicted from the size distribution of phytoplankton. This occurs because, under equilibrium conditions, the factors regulating the relative growth and loss rates of the different populations (and hence also the net metabolism of the community)—i.e., competitive aptitude for nutrients and light uptake, sinking rate, predator-prey interactions, susceptibility to grazing control, and DOM exudation—are all dependent on cell size. A combination of the adequate representation of the structure of planktonic food webs by the size structure of phytoplankton and the existence of a link between community structure and food web fluxes in functional communities (e.g., Hairston and Hairston 1993) has enabled several conceptual models to relate the percentage of export (Legendre and Lefevre 1989; Tremblay and Legendre 1994; Legendre and Rassoulzadegan 1996; Boyd and Newton 1999) or new production (Tremblay et al. 1997) to the relative dominance of particular food webs. Predictions of these models have been frequently satisfied in the field (e.g., Heiskanen et al. 1996; Pesant et al. 1998; Tamigneaux et al. 1999; Pesant et al. 2000), except when the scale of study did not match that of the functioning of the ecosystem (e.g., Rivkin et al. 1996). Within this conceptual framework, but by simply reversing the logic, we have investigated the representativeness of our data set by analyzing the relation between community structure (as summarized by phytoplankton size) and ecological energetics (summarized by NCP) in our sampled communities.

The latitudinal variation of the euphotic zone integrated percentage of particulate carbon incorporated by phytoplankton $< 2 \mu\text{m}$ ($\% \text{PO}^{14}\text{CP} < 2 \mu\text{m}$) and integrated NCP shows a clear inverse relationship along the AMT-6 transect (Fig. 7A). Such a significant relationship is described by the equation (reduced major axis) $\text{NCP} = -276.5 \log (\% \text{PO}^{14}\text{CP} < 2 \mu\text{m}) + 972.9$, $r^2 = 0.761$, $n = 21$, $P < 0.0001$ (Fig. 7B). This relationship does not reveal whether community structure affects plankton GPP:CR balance, because that could simply result from the respective covariation of both NCP and phytoplankton size with total GPP. What such a strong relationship between trophic structure and functioning does suggest is that our data are representative of different ecological communities, and, specifically, that the plankton communities from oligotrophic and eutrophic provinces were functionally distinct. This is an important observation

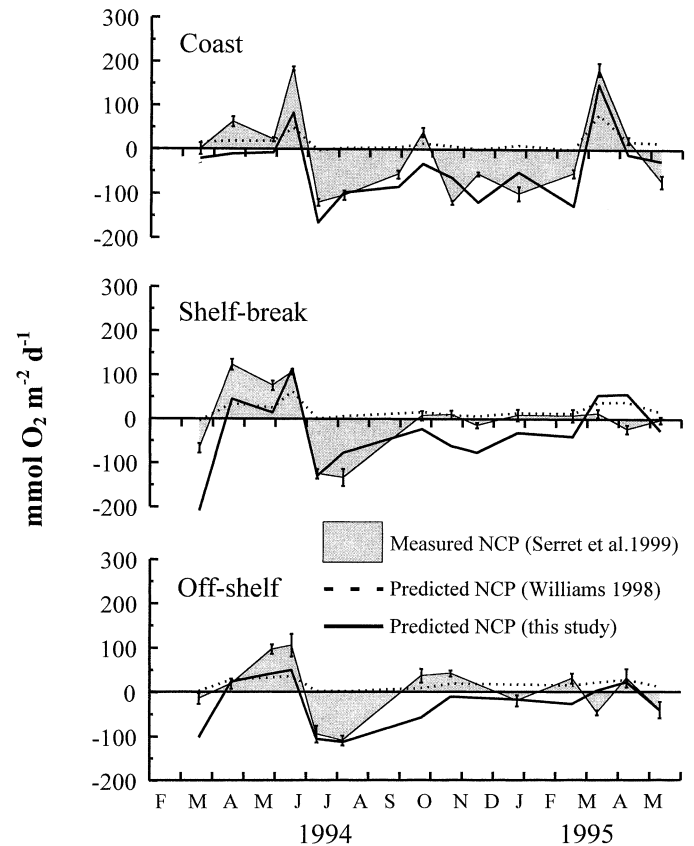


Fig. 9. Seasonal variation in euphotic zone integrated rates of NCP at three stations (~ 50 , 250, and 1,000 m depth) across the coastal transitional zone of the southern Bay of Biscay. Shaded trend, measured rates (\pm SE). Dashed line, NCP rates predicted from GPP by the model of Williams (1998): $\Sigma R = 0.73 (\Sigma \text{GPP}) + 4.57$, $r^2 = 0.536$, $P = 0.02$, $n = 65$, where ΣR and ΣGPP are the integrated rates of R and GPP, respectively. Estimation of O_2 GPP derives from the sum of measured NCP and DCR (see Materials and Methods); hence, it is not independent of either of them. Nevertheless, for the comparative test presented here, we have followed an analogous approach to Williams (1998): integrated NCP (solid line) was predicted from GPP by use of the empirical relationship between integrated GPP and NCP along the AMT-6 transect: $\text{NCP} = 63.434 \times \text{GPP}^{0.34} - 300$, $r^2 = 0.71$, $n = 19$, $P < 0.001$.

that will help us to interpret our results of community metabolism.

GPP: CR relationships: the influence of community structure—Because the derivation of GPP and CR from in vitro changes in dissolved oxygen in this study is almost identical to that employed in Williams (1998), a direct comparison can be made, thus overcoming the interpretative problems associated with comparing different analytical methods (i.e., the ^{14}C technique used in del Giorgio et al. 1997 and Duarte et al. 1999). Using the same method of data analysis as Williams (1998), we found that integrated DCR was remarkably constant over a range of integrated GPP of almost three orders of magnitude (Fig. 8A), which agrees with the results of del Giorgio et al. (1997) and supports their conclusion that microbial CR exceeds GPP in unproductive systems (see

also Duarte et al. 1999). We found that, at integrated rates of GPP below $\sim 100 \text{ mmol O}_2 \text{ m}^{-2} \text{ d}^{-1}$, heterotrophy prevailed. This contrasts with the results of Williams (1998), who, from data collected from five open ocean regions derived the point of metabolic balance to be $16.7 \text{ mmol O}_2 \text{ m}^{-2} \text{ d}^{-1}$. Figure 8A also shows that the constancy of integrated DCR only occurs through the sampling of both distinct eutrophic (black circles) and oligotrophic (open triangles and circles) communities, which suggests that our discrepancy with Williams (1998) may result from a different coverage of plankton communities. Of the data sets examined by Williams (1998), only those from the North Pacific Central Gyre may be considered as representing real oligotrophic communities, but these were only 5 out of a total of 65 profiles used in the analysis.

Comparison of the low GPP parts of the integrated GPP:DCR plots in Williams (1998) and the present study confirms that such a discrepancy does not arise from the different range of GPP. Of his 33 stations with integrated GPP $< 100 \text{ mmol O}_2 \text{ m}^{-2} \text{ d}^{-1}$ (range, $\sim 25\text{--}100 \text{ mmol O}_2 \text{ m}^{-2} \text{ d}^{-1}$) only 5 values of DCR were $> 100 \text{ mmol O}_2 \text{ m}^{-2} \text{ d}^{-1}$, and the average DCR was $\sim 55 \text{ mmol O}_2 \text{ m}^{-2} \text{ d}^{-1}$ (fig. 2a in Williams 1998). Conversely, in our data set, five out of a total of six stations within the same range of integrated GPP ($25\text{--}100 \text{ mmol O}_2 \text{ m}^{-2} \text{ d}^{-1}$) had integrated DCR $> 100 \text{ mmol O}_2 \text{ m}^{-2} \text{ d}^{-1}$, and the average DCR was $141 \pm 18 \text{ mmol O}_2 \text{ m}^{-2} \text{ d}^{-1}$; the only station with DCR $< 100 \text{ mmol O}_2 \text{ m}^{-2} \text{ d}^{-1}$ (GPP = 95 ± 8 , DCR = $75 \pm 6 \text{ mmol O}_2 \text{ m}^{-2} \text{ d}^{-1}$) corresponded to the Benguela upwelling region. This observation is sustained when all our stations with GPP $< 100 \text{ mmol O}_2 \text{ m}^{-2} \text{ d}^{-1}$ are considered: eight of nine stations had DCR $> 100 \text{ mmol O}_2 \text{ m}^{-2} \text{ d}^{-1}$ (average DCR $146 \pm 12 \text{ mmol O}_2 \text{ m}^{-2} \text{ d}^{-1}$).

Williams (1998) found that the water-column integration of his volumetric data tended to move the GPP:DCR relationship toward the 1:1 line, whereas our data show exactly the opposite trend (Fig. 8A,B). The explanation given by Williams (1998) for the change in the slope between his volumetric and areal GPP:DCR relationships was the compensation of imbalances over the vertical profile, but in our data from oligotrophic provinces, heterotrophy prevailed throughout the water column (Figs. 6 and 8B). Although the ranges of volumetric GPP overlap between oligotrophic and eutrophic environments (Fig. 8B), vertical integration tends to segregate the values from the different regions (Fig. 8A). That is, volumetric data combines low GPP values from two very different origins: functionally oligotrophic communities and locally growth-limited eutrophic communities. In eutrophic regions, heterotrophic balances at some depths tend to be compensated by autotrophic balances at other depths (usually near the surface); thus, the integrated value tends toward metabolic balance (Williams 1998) (Fig. 8A). However, this does not occur in oligotrophic regions, so inclusion of data from oligotrophic communities in our analysis causes the observed constancy of integrated DCR.

Such imbalances in the ETRA and NAST require allochthonous supplies of organic matter. Various studies have shown a seasonal accumulation of dissolved organic carbon (DOC) in the upper waters of both open ocean (Hansell and Carlson 1998) and coastal ecosystems (Álvarez-Salgado et

al. 2001). The possible fate for accumulated DOC is delayed local consumption, local downward export associated with winter convective mixing or horizontal transport, or a combination of any of these. Hence, within the winter mixed layer, there will be areas where or seasons when net consumption of allochthonous DOC must take place to enable the DOC concentrations to return to those present before the seasonal accumulation. Whenever such consumption occurs concurrently with low local primary production, a net heterotrophic metabolism can develop. Net heterotrophy measured during the summer in some temperate seas therefore has been explained as a result of the consumption during the oligotrophic season of DOC accumulated during the preceding spring bloom (Serret et al. 1999 and references therein). Hansell and Carlson (1998) have shown that DOC accumulation at the BATS station in the Sargasso Sea (NAST-W) may reach 59%–70% of the spring bloom NCP; however, it is unlikely that organic matter locally accumulated in the unproductive NAST-E and ETRA can sustain the rates of net heterotrophy presented here. Nonetheless, Hansell et al. (1995) measured rates of DOC mineralization exceeding concurrent primary production rates in the Sargasso Sea and concluded that either GPP had been underestimated or that previously produced DOC was supporting periods of net heterotrophy in this region. Rates of DOC mineralization in the Sargasso Sea were $\sim 0.45 \text{ mmol C m}^{-3} \text{ d}^{-1}$ (Hansell et al. 1995), whereas, following the method of Hansell and Carlson (1998), the net consumption of DOC in the upper 250 m of the BATS station after the 1995 spring bloom can be estimated to be $\sim 0.2 \text{ mmol C m}^{-3} \text{ d}^{-1}$. These values represent $\sim 45\%$ and 20% of the negative NCP rates in the euphotic zone of the NAST-E presented here. In the Azores Front region, Doval et al. (2001) have measured rates of DOC accumulation in the upper 100 m during August 1998 of $0.47 \text{ mmol C m}^{-3} \text{ d}^{-1}$, i.e., $\sim 50\%$ of our negative NCP rates in the NAST-E. However, a significant contribution of photoheterotrophy to community metabolism, by reducing the respiratory energy requirements in bacterial DOM assimilation (Béjà et al. 2000; Kolber et al. 2000), would further increase the demand of DOM in relation to our measurements of O_2 consumption. A lateral input of DOC to the eastern Atlantic from the neighboring upwelling system off the northwest African coast (Hansell and Carlson 1998; Álvarez-Salgado et al. 2001), aeolian inputs (Cornell et al. 1995), and possibly river discharge are also potentially important in the ETRA and NAST provinces. The limited quantitative information on these large-scale and episodic supply mechanisms means that it is difficult to completely account for the carbon demand required for the NCP data presented here.

Plankton community structure influences net ecosystem metabolism: constraining the global estimation of NCP—We have shown that volumetric and areal GPP:DCR relationships change when data from characteristic oligotrophic communities are included, irrespective of the ranges of GPP. We therefore suggest that community structure, and not only the amount of photosynthesis, influences the degree of heterotrophy of marine plankton ecosystems. Hypotheses derived from empirical relationships can only be tested through

their predictions (e.g., Peters 1991). We have hence compared the predictive ability of the integrated GPP:CR empirical relationship presented here with that in Williams (1998). These two empirical relationships, which differ most in the range of communities sampled but not in the magnitude of GPP, are used to predict the behavior of systems environmentally similar but taxonomically, geographically, and temporally different from those included in either model derivation (Tonn et al. 1990). Given that our empirical model is based on the large-scale spatial variability of NCP, its most rigorous test would be the prediction of the temporal variation of NCP at a single location (Burke et al. 1997). We have used data from the only comprehensive seasonal study of euphotic zone NCP found in the literature (Serret et al. 1999) (Fig. 9). The prediction of our model, derived from a wide range of distinct plankton communities, fairly reproduces the measured seasonal cycle of integrated NCP at three stations across the coastal transitional zone of the southern Bay of Biscay, and in particular, the characteristic spring-summer auto-heterotrophic transition. By contrast, the model based on a similar range of GPP, but a single type of community (Williams 1998), failed to predict any net heterotrophy throughout the entire seasonal cycle, even during the summer, when characteristic oligotrophic communities prevail in the region. Furthermore, a GPP:DCR relationship close to 1:1 (Williams 1998) would require disproportionately high values of GPP to justify the measured rates of NCP during, e.g., the northern Atlantic spring phytoplankton bloom (e.g., Kiddon et al. 1995; Serret et al. 1999). Following the empirical GPP:DCR relationship in Williams (1998), integrated rates of GPP close to $760 \text{ mmol O}_2 \text{ m}^{-2} \text{ d}^{-1}$ ($>9 \text{ g C m}^{-2} \text{ d}^{-1}$) would be necessary to sustain measured NCP rates of $\sim 200 \text{ mmol O}_2 \text{ m}^{-2} \text{ d}^{-1}$ (Serret et al. 1999).

We therefore suggest that food web fluxes can be predicted in pelagic ecosystems, despite their enormous taxonomic and functional complexity and diversity, only when proper consideration of the influence of community structure on trophic dynamics is made—that is, when the model used is derived from a representative range of community structures. This is consistent with analyses of the control of ecological efficiencies by trophic structure in freshwater and terrestrial ecosystems (Hairton and Hairton 1993) and with microcosm experiments that revealed an increase in decomposition rates with the complexity of aquatic microbial webs (McGrady-Steed et al. 1997; Petchey et al. 1999). Such a trophic constraint on empirical GPP:CR relationships may help us understand the functional relationship between food web organization and net metabolism in pelagic ecosystems and should be considered for interpretation of NCP predictions. Although our results indicate that net heterotrophy prevails where total GPP $< \sim 100 \text{ mmol O}_2 \text{ m}^{-2} \text{ d}^{-1}$ and the %PO¹⁴CP attributable to $< 2\text{-}\mu\text{m}$ cells exceeds 33%, they also highlight the difficulties in extrapolating observations beyond the studied range of pelagic ecosystems. This precludes an estimation of the metabolic balance of the global ocean from the empirical GPP:CR relationship presented here, which is based on a spring-summer sampling of systems located in either the marginal regions of the subtropical gyres or close (150–500 nm) to highly productive coastal provinces.

References

- AIKEN J., AND OTHERS. 2000. The Atlantic Meridional Transect: Overview and synthesis of data. *Prog. Oceanogr.* **45**: 257–312.
- ÁLVAREZ-SALGADO, X. A., J. GAGO, B. MÍGUEZ, AND F. F. PÉREZ. 2001. Net ecosystem production of dissolved organic carbon in a coastal upwelling system: The Ría de Vigo, Iberian margin of the North Atlantic. *Limnol. Oceanogr.* **46**: 135–147.
- BÉJA, O., AND OTHERS. 2000. Bacterial rhodopsin: Evidence for a new type of phototrophy in the sea. *Science* **289**: 1902–1906.
- BENSON, B. B., AND D. KRAUSE JR. 1984. The concentration and isotopic fractionation of oxygen dissolved in freshwater and seawater in equilibrium with the atmosphere. *Limnol. Oceanogr.* **29**: 620–632.
- BLIGHT, S. P., T. L. BENTLEY, D. LEFEVRE, C. ROBINSON, R. RODRIGUES, J. ROWLANDS, AND P. J. LE B. WILLIAMS. 1995. Phasing of autotrophic and heterotrophic plankton metabolism in a temperate coastal ecosystem. *Mar. Ecol. Prog. Ser.* **128**: 61–75.
- BOYD, P. W., AND P. P. NEWTON. 1999. Does planktonic community structure determine downward particulate organic carbon flux in different oceanic provinces? *Deep-Sea Res. I* **46**: 63–91.
- BURKE, I. C., W. K. LAUENROTH, AND W. J. PARTON. 1997. Regional and temporal variation in net primary production and nitrogen mineralization in grasslands. *Ecology* **78**: 1330–1340.
- CHAPMAN, P., AND L. V. SHANNON. 1985. The Benguela ecosystem. Part II: Chemistry and related processes. *Oceanogr. Mar. Biol. Annu. Rev.* **23**: 183–251.
- CORNELL, S., A. RENDELL, AND T. JICKELLS. 1995. Atmospheric inputs of dissolved organic nitrogen to the oceans. *Nature* **376**: 243–246.
- DEL GIORGIO, P. A., AND J. J. COLE. 1997. Photosynthesis or planktonic respiration? Reply. *Nature* **388**: 132.
- , AND A. CIMBLERIS. 1997. Respiration rates in bacteria exceed phytoplankton production in unproductive systems. *Nature* **385**: 148–151.
- DOVAL, M. D., X. A. ÁLVAREZ-SALGADO, AND F. F. PÉREZ. 2001. Organic matter distributions in the Eastern North Atlantic-Azores Front Region. *J. Mar. Syst.* **30**: 33–49.
- DUARTE, C. M., AND S. AGUSTÍ. 1998. The CO₂ balance of unproductive aquatic ecosystems. *Science* **281**: 234–236.
- , S. AGUSTÍ, P. A. DEL GIORGIO, AND J. J. COLE. 1999. Regional carbon imbalances in the oceans. *Response. Science* **284**: 1735b.
- GEIDER, R. J. 1992. Respiration: Taxation without representation?, p. 333–360. *In* P. G. Falkowski and A. D. Woodhead [eds.], Primary production and biogeochemical cycles in the sea. Plenum.
- . 1997. Photosynthesis or planktonic respiration? *Nature* **388**: 132.
- HAIRSTON, N. G. JR., AND N. G. HAIRSTON SR. 1993. Cause-effect relationships in energy flow, trophic structure, and interspecific interactions. *Am. Nat.* **142**: 379–411.
- HANSELL, D. A., N. R. BATES, AND K. GUNDERSEN. 1995. Mineralization of dissolved organic carbon in the Sargasso Sea. *Mar. Chem.* **51**: 201–212.
- , AND C. A. CARLSON. 1998. Net community production of dissolved organic carbon. *Global Biogeochem. Cycles* **12**: 443–453.
- HEISKANEN, A.-S., T. TAMMINEN, AND K. GUNDERSEN. 1996. Impact of planktonic food web structure on nutrient retention and loss from a late summer pelagic system in the coastal northern Baltic Sea. *Mar. Ecol. Prog. Ser.* **145**: 195–208.
- JOINT, I., A. POMROY, G. SAVIDGE, AND P. BOYD. 1993. Size-fractionated primary productivity in the northeast Atlantic in May–July 1989. *Deep-Sea Res. II* **40**: 423–440.

- KIDDON, J., M. L. BENDER, AND J. MARRA. 1995. Production and respiration in the 1989 North Atlantic spring bloom: An analysis of irradiance-dependent changes. *Deep-Sea Res.* **42**: 553–576.
- KJØRBOE, T. 1993. Turbulence, phytoplankton cell size, and the structure of pelagic food webs. *Adv. Mar. Biol.* **29**: 1–72.
- KOLBER, Z. S., C. L. VAN DOVER, R. A. NIEDERMAN, AND P. G. FALKOWSKI. 2000. Bacterial photosynthesis in surface waters of the open ocean. *Nature* **407**: 177–179.
- LEGENBRE, L., M. GOSSELIN, H. J. HIRCHE, G. KATTNER, AND G. ROSENBERG. 1993. Environmental control and potential fate of size-fractionated phytoplankton production in the Greenland Sea (75°N). *Mar. Ecol. Prog. Ser.* **98**: 297–313.
- , AND J. LEFEVRE. 1989. Hydrodynamical singularities as controls of recycled versus export production in the oceans, p. 44–63. *In* W. H. Berger, V. S. Smetacek, and G. Wefer [eds.], *Productivity of the oceans: Present and past*. Wiley.
- , AND ———. 1991. From individual plankton cells to pelagic marine ecosystems and to global biogeochemical cycles, p. 261–300. *In* S. Demmers [ed.], *Particle analysis in oceanography*. Springer.
- , AND F. RASSOULZADEGAN. 1996. Food-web mediated export of biogenic carbon in oceans: Hydrodynamic control. *Mar. Ecol. Prog. Ser.* **145**: 179–193.
- LONGHURST, A. 1998. *Ecological geography of the sea*. Academic.
- LUTJEHARMS, J. R. E., AND J. M. MEEUWIS. 1987. The extent and variability of south-east Atlantic upwelling. *S. Afr. J. Mar. Sci.* **5**: 51–62.
- MARAÑÓN, E., P. HOLLIGAN, M. VARELA, B. MOURIÑO, AND A. J. BALE. 2000. Basin-scale variability of phytoplankton biomass, production and growth in the Atlantic Ocean. *Deep-Sea Res. I* **47**: 825–857.
- MCGRADY-STEED, J., P. M. HARRIS, AND P. J. MORIN. 1997. Biodiversity regulates ecosystem predictability. *Nature* **390**: 162–165.
- MICHAELS, A. F., AND A. H. KNAP. 1996. Overview of the U.S. JGOFS Bermuda Atlantic Time-series Study and the Hydrostation S program. *Deep-Sea Res. II* **43**: 157–198.
- MILLER, J. C., AND J. N. MILLER. 1988. *Statistics for analytical chemistry*, 2nd ed. Ellis Horwood Limited.
- MOLONEY, C. L., AND J. G. FIELD. 1991. The size-based dynamics of plankton food webs. I. A simulation model of carbon and nitrogen flows. *J. Plankton Res.* **13**: 1003–1038.
- MOREL, A., D. ANTOINE, M. BABIN, AND Y. DANDONNEAU. 1996. Measured and modeled primary production in the northeast Atlantic (EUMELI JGOFS program): The impact of natural variations in photosynthetic parameters on model predictive skill. *Deep-Sea Res. I* **43**: 1273–1304.
- NAJJAR, R. G., AND R. F. KEELING. 1997. Analysis of the mean annual cycle of the dissolved oxygen anomaly in the World Ocean. *J. Mar. Res.* **55**: 117–151.
- NIELSEN, T. G., AND B. HANSEN. 1995. Plankton community structure and carbon cycling on the western coast of Greenland during and after the sedimentation of a diatom bloom. *Mar. Ecol. Prog. Ser.* **125**: 239–257.
- OUDOT, C. 1989. O₂ and CO₂ balances approach for estimating biological production in the mixed layer of the tropical Atlantic Ocean (Guinea Dome area). *J. Mar. Res.* **47**: 385–409.
- PETERS, R. H. 1991. *A critique for ecology*. Cambridge Univ. Press.
- PESANT, S., AND OTHERS. 1998. Pathways of carbon cycling in the euphotic zone: The fate of large-sized phytoplankton in the Northeast Water Polynya. *J. Plankton Res.* **20**: 1267–1291.
- , L. LEGENDRE, M. GOSSELIN, P. K. BJORNSEN, L. FORTIER, J. MICHAUD, AND T. G. NIELSEN. 2000. Pathways of carbon cycling in marine surface waters: The fate of small-sized phytoplankton in the Northeast Water Polynya. *J. Plankton Res.* **22**: 779–801.
- PETCHEY, O. L., P. T. MCPHEARSON, T. M. CASEY, AND P. J. MORIN. 1999. Environmental warming alters food-web structure and ecosystem function. *Nature* **402**: 69–72.
- PITCHER, G. C., P. C. BROWN, AND B. A. MITCHELL-INNES. 1992. Spatio-temporal variability of phytoplankton in the Southern Benguela upwelling system, p. 439–456. *In* A. I. L. Payne, K. H. Brink, K. H. Mann, and R. Hilborn [eds.], *Benguela trophic functioning*. S. Afr. J. Mar. Sci. **12**.
- POMEROY, L. R., AND W. J. WIEBE. 1993. Energy sources for microbial food webs. *Mar. Microb. Food Webs* **7**: 101–118.
- RIVKIN, R. B., AND OTHERS. 1996. Vertical flux of biogenic carbon in the ocean: Is there food web control? *Science* **272**: 1163–1166.
- SARMIENTO, J. L., AND SIEGENTHALER, U. 1992. New production and the global carbon cycle, p. 317–332. *In* P. G. Falkowski and A. D. Woodhead [eds.], *Primary productivity and biogeochemical cycles in the sea*. Plenum.
- SERRET, P., E. FERNÁNDEZ, J. A. SOSTRES, AND R. ANADÓN. 1999. Seasonal compensation of plankton production and respiration in a temperate sea. *Mar. Ecol. Prog. Ser.* **187**: 43–57.
- SHANNON, L. V., J. J. AGENBAG, AND M. E. L. BUYS. 1987. Large and mesoscale features of the Angola/Benguela Front. *S. Afr. J. Mar. Sci.* **5**: 11–34.
- , AND S. C. PILLAR. 1986. The Benguela ecosystem. Part III. Plankton. *Oceanogr. Mar. Biol. Annu. Rev.* **24**: 65–170.
- SHERR, E. B., AND B. F. SHERR. 1996. Temporal offset in oceanic production and respiration processes implied by seasonal changes in atmospheric oxygen: The role of heterotrophic microbes. *Aquat. Microb. Ecol.* **11**: 91–100.
- SMITH, S. V., AND J. T. HOLLIBAUGH. 1997. Annual cycle and interannual variability of ecosystem metabolism in a temperate climate embayment. *Ecol. Monogr.* **67**: 509–533.
- STRAMMA, L., AND F. SCHOTT. 1999. The mean flow field of the tropical Atlantic Ocean. *Deep-Sea Res. II* **46**: 279–303.
- TAMIGNEAUX, E., L. LEGENDRE, B. KLEIN, AND M. MINGELBIER. 1999. Seasonal dynamics and potential fate of size-fractionated phytoplankton in a temperate nearshore environment (western Gulf of St. Lawrence, Canada). *Estuar. Coast. Shelf Sci.* **48**: 253–269.
- TONN, W. M., J. J. MAGNUSON, M. RASK, AND J. TOIVONEN. 1990. Intercontinental comparison of small-lake fish assemblages: The balance between local and regional processes. *Am. Nat.* **136**: 345–375.
- TREMBLAY, J. E., B. KLEIN, L. LEGENDRE, R. B. RIVKIN, AND J. C. THERRIAULT. 1997. Estimation of the f-ratios in oceans based on phytoplankton size structure. *Limnol. Oceanogr.* **42**: 595–601.
- , AND L. LEGENDRE. 1994. A model for the size-fractionated biomass and production of marine phytoplankton. *Limnol. Oceanogr.* **39**: 2004–2014.
- WILLIAMS, P. J. LE B. 1993. On the definition of plankton production terms, p. 9–19. *In* W. K. W. Li and S. Y. Maestrini [eds.], *Measurement of primary production from the molecular to the global scale*. ICES Mar. Sci. Symp. **197**.
- . 1998. The balance of plankton respiration and photosynthesis in the open oceans. *Nature* **394**: 55–57.
- , AND D. G. BOWERS. 1999. Regional carbon imbalances in the oceans. *Science* **284**: 1735b.
- , AND N. W. JENKINSON. 1982. A transportable microprocessor-controlled precise Winkler titration suitable for field station and shipboard use. *Limnol. Oceanogr.* **27**: 576–584.

Received: 28 December 2000

Accepted: 19 June 2001

Amended: 13 July 2001